JCTC Journal of Chemical Theory and Computation

ARTICLE

pubs.acs.org/JCTC

Pairwise Long-Range Compensation for Strongly Ionic Systems

Seyit Kale[†] and Judith Herzfeld[*,‡]

[†]Graduate Program in Biophysics and Structural Biology, Brandeis University, Waltham, Massachusetts 02454, United States

[‡]Department of Chemistry, Brandeis University, Waltham, Massachusetts 02454, United States

ABSTRACT: We propose a pairwise compensation method for long-range electrostatics, as an alternative to traditional infinite lattice sums. The approach represents the third generation in a series beginning with the shifted potential corresponding to counterions surrounding a cutoff sphere. That simple charge compensation scheme resulted in pairwise potentials that are continuous at the cutoff, but forces that are not. A second-generation approach modified both the potential and the force such that both are continuous at the cutoff. Here, we introduce another layer of softening such that the derivative of the force is also continuous at the cutoff. In strongly ionic liquids, this extension removes structural artifacts associated with the earlier pairwise compensation schemes and provides results that compare well with Ewald sums.

INTRODUCTION

Accurate treatment of long-range electrostatics is crucial for the reliability of molecular simulations.[1] The slow convergence of the $1/r$ term precludes termination at a practical cutoff distance,[2−4] as is typically done, e.g., for van der Waals interactions.[5,6] A widely accepted solution imposes an infinitely repeating lattice that allows the slowly converging Coulomb sum to be separated into a sum that converges rapidly in real space and another that converges rapidly in reciprocal space.[7] Collectively known as Ewald or lattice summations,[8−11] these methods rely on the suitability of the infinite lattice.

A more intuitive alternative has been proposed by Wolf et al. in a study of Madelung energies in perfect crystals.[12] In their approach, the electrostatic pair potentials are shifted by their value at the cutoff distance:

$$U_{SP}(r_{ij}) = \begin{cases} U(r_{ij}) - U(r_c) & r_{ij} \le r_c \\ 0 & r_{ij} > r_c \end{cases} \quad (1)$$

$$F_{SP}(r_{ij}) = \begin{cases} -\dfrac{dU(r_{ij})}{dr} & r_{ij} \le r_c \\ 0 & r_{ij} > r_c \end{cases} \quad (2)$$

where U is the original potential, dU/dr is its derivative with respect to distance, r_{ij} is the distance between particles i and j, and r_c is the distance cutoff, typically chosen in the range of 9−12 Å. Physically, this adjustment amounts to placing counterions on the cutoff sphere. Mathematically, this adjustment corresponds to the previously published shifted potential (SP), which achieves continuity at the cutoff for potentials of any form.[13]

In this scheme, the force (eq 2) does not "feel" the charge neutralization and remains discontinuous at the cutoff (Figure 1). Wolf et al.[12] addressed this issue by applying damping, and Zahn et al.[14] subsequently revised Wolf's damping to achieve energy conservation in MD simulations. However, damping introduces an additional arbitrary parameter. A more straightforward approach to energy conservation is the shifted force (SF),[13,15] which meets two continuity requirements at the cutoff boundary, i.e., for both the potential and its derivative (similar to the boundary conditions applied to the Poisson−Boltzmann calculation in reaction field methods, but without the need to assume a uniform continuum with known dielectric constant beyond the cutoff[16−18]):

$$U_{SF}(r_{ij}) = \begin{cases} U(r_{ij}) - U(r_c) - (r_{ij} - r_c)\dfrac{dU(r_c)}{dr} & r_{ij} \le r_c \\ 0 & r_{ij} > r_c \end{cases} \quad (3)$$

$$F_{SF}(r_{ij}) = \begin{cases} -\dfrac{dU(r_{ij})}{dr} + \dfrac{dU(r_c)}{dr} & r_{ij} \le r_c \\ 0 & r_{ij} > r_c \end{cases} \quad (4)$$

Rigorous tests on this shifted force method have been reported by Fennell and Gezelter.[19] On the basis of comparisons with Ewald energies and forces in SPC/E water[20] and in high temperature molten salts, they conclude that force shifting can be a viable alternative to lattice sums. More recently, Toxvaerd and Dyre reported that SF potentials permit smaller cutoffs in weakly bound systems.[6]

However, problems arise when we apply SF to an unusual ionic liquid of "molecules" that are inherently polarizable and reactive. In this model, molecules comprise charged and independently mobile atomic cores that are surrounded by fully charged and independently mobile valence electron pairs.[21] According to this "LEWIS" construct, a water molecule, e.g., is composed of seven independently mobile particles: a +6 charged oxygen core, two +1 charged protons, and four −2 charged electron pairs (Figure 2, inset). These charges are an order of magnitude larger than the partial charges of typical empirical force fields. In this unusual ionic liquid, SF does

Received: June 9, 2011
Published: September 15, 2011

dx.doi.org/10.1021/ct200392u | *J. Chem. Theory Comput.* 2011, 7, 3620–3624

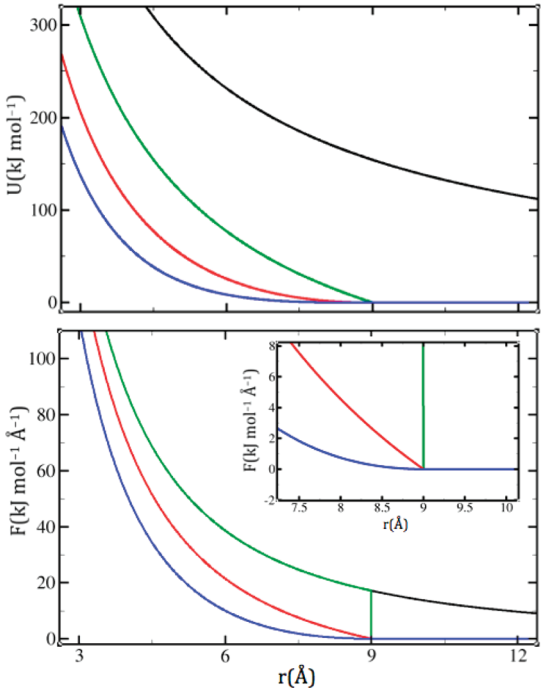

Figure 1. Three different levels of shifting on a purely electrostatic potential $U = 1/r$ (top) and its force $F = 1/r^2$ (bottom), as they approach a cutoff of 9 Å. The unmodified potential and force are shown in black, the SP in green, the SF in red, and the SFG in blue. In b, the inset shows a magnified view of the cutoff region. Note that in both SF and SFG the energies go smoothly to zero, whereas the force goes smoothly to zero only in SFG.

better than SP but still produces significant structural artifacts (Figure 2). To address this problem, we take the approach one step further, by shifting the gradient of the force to make it continuous at the cutoff and adjusting the force and potential accordingly:

$$U_{\mathrm{SFG}}(r_{ij}) = \begin{cases} U(r_{ij}) - U(r_c) - (r_{ij} - r_c)\dfrac{\mathrm{d}U(r_c)}{\mathrm{d}r} - \dfrac{1}{2}(r_{ij} - r_c)^2 \dfrac{\mathrm{d}^2U(r_c)}{\mathrm{d}r^2} & r_{ij} \le r_c \\ 0 & r_{ij} > r_c \end{cases} \tag{5}$$

$$F_{\mathrm{SFG}}(r_{ij}) = \begin{cases} -\dfrac{\mathrm{d}U(r_{ij})}{\mathrm{d}r} + \dfrac{\mathrm{d}U(r_c)}{\mathrm{d}r} + (r_{ij} - r_c)\dfrac{\mathrm{d}^2U(r_c)}{\mathrm{d}r^2} & r_{ij} \le r_c \\ 0 & r_{ij} > r_c \end{cases} \tag{6}$$

Here, SFG stands for *shifted force gradient*, and $\mathrm{d}^2U/\mathrm{d}r^2$ denotes the second derivative of potential with respect to distance. Note that the second derivatives appear as constants, and they need to be evaluated only once per type of interaction. Since the force remains the exact derivative of the potential, energy is still conserved in molecular dynamics (MD) simulations.[6]

We should note that a general shifting scheme was discussed long ago by Levitt et al.[22] in the form of a truncated Taylor series

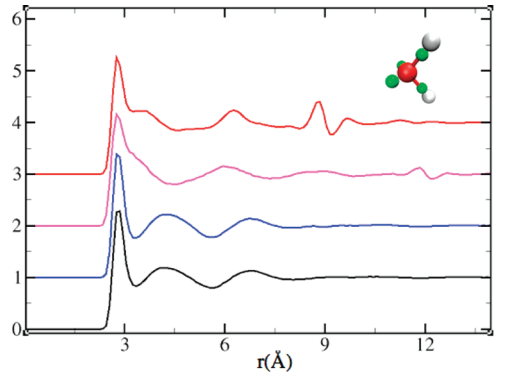

Figure 2. The smooth particle mesh Ewald (SPME) oxygen−oxygen radial distribution function of LEWIS water[21] compared to the (vertically translated) results obtained using SFG with $r_c = 9$ Å in blue; SF with $r_c = 12$ Å in magenta; and SF with $r_c = 9$ Å in red. The inset shows one molecule of LEWIS water: the oxygen ion is rendered in red, protons in white, and electron pairs in green.

expansion:

$$U_{n\text{-shifted}}(r_{ij}) = \begin{cases} U(r_{ij}) - U(r_c) - \displaystyle\sum_{m=1}^{n} \frac{1}{m!}(r_{ij} - r_c)^m \frac{\mathrm{d}^m U(r_c)}{\mathrm{d}r^m} & r_{ij} \le r_c \\ 0 & r_{ij} > r_c \end{cases} \tag{7}$$

Levitt et al.[22] explored both the $n = 1$ case (corresponding to SF) and the $n = 2$ case (corresponding to SFG) and concluded that the former provides a better electrostatics description in weakly to mildly ionic systems, such as aqueous solutions of biological macromolecules. They also argued that force shifting, i.e., $n = 1$, has little influence on a hydrogen bond that is modeled by partial charges on atom centers. Here, we show that in cases of extreme ionicity, as encountered in novel or rare model systems, these conclusions may be challenged, and $n > 1$ orders of shifting can become necessary for proper long-range electrostatics.

COMPUTATIONAL DETAILS

All MD simulations were performed with Gromacs software[23] version 4.5.3 and analyzed using Gromacs and VMD[24] (version 1.8.7). Potentials were introduced as user tabulated functions with a distance increment of $\Delta r = 0.005$ Å. Ewald sums were calculated using Gromacs' smooth particle mesh Ewald (SPME), implemented with fourth order spline interpolation and a tolerance of 10^{-5}. In these runs, the non-Coulombic terms were handled as in eqs 5 and 6 with $r_c = 9$ Å. Since these terms decay rapidly, their effect in the long-range was small compared to the Coulomb term. Following the approach of Fennell and Gezelter,[19] we take the Ewald results as our reference.

The sodium chloride simulations used the Charmm27 force field,[26,27] such that the interaction between ions i and j is

$$U_{ij} = \frac{q_i q_j}{4\pi\varepsilon_0 r_{ij}} + \varepsilon_{ij}^{\min}\left[\left(\frac{R_{ij}^{\min}}{r_{ij}}\right)^{12} - 2\left(\frac{R_{ij}^{\min}}{r_{ij}}\right)^{6}\right] \tag{8}$$

where $\varepsilon_{ij}^{\min} = (\varepsilon_i^{\min}\,\varepsilon_j^{\min})^{1/2}$ and $R_{ij}^{\min} = (R_i^{\min} + R_j^{\min})/2$ and the parameter values are listed in Table 1.

Simulations were run at 2000 K where the model potentials predict a molten liquid that still exhibits extensive structural order.

Table 1. Charges and Lennard-Jones Parameters Used in NaCl Simulations[25−27]

	q (e)	R^{min} (Å)	ε^{min} (kcal/mol)
Na^+	1.00	2.7275	−0.0469
Cl^-	−1.00	3.8164	−0.0300

Table 2. Charges and Lennard-Jones Parameters Used in $ThCl_4$ Simulations (as found in the Gromacs 4.5.3 release)

	q (e)	ρ (Å)	ε (kJ/mol)
Th^{4+}	4.00	3.30000	0.209200
Cl^-	−1.00	4.41724	0.492833

All simulations were in the NPT ensemble. The temperature was maintained using stochastic velocity rescaling[28] with a time constant of 0.1 ps. Pressures were maintained at 1 atm using an isotropic Berendsen barostat[29] with a time constant of 10 ps and compressibility of 4.5×10^{-5} bar^{-1}. All NaCl runs began with conjugate gradient energy minimization of a perfect simple cubic 16 × 16 × 16 crystal with a lattice spacing of 2.0 Å. The integration time step was 2 fs, and neighbor lists were updated very frequently (every five steps) to avoid possible artifacts. Neighbor list radii were 2 Å longer than the cutoffs. Each simulation ran for 1 ns, and the last 800 ps were used for analysis. Coordinates were saved every other picosecond.

Thorium(IV) tetrachloride simulations used the OPLS-AA force field[30,31] such that the interaction between ions i and j is given by

$$U_{ij} = \frac{q_i q_j}{4\pi\varepsilon_0 r_{ij}} + 4\varepsilon_{ij}\left[\left(\frac{\rho_{ij}}{r_{ij}}\right)^{12} - \left(\frac{\rho_{ij}}{r_{ij}}\right)^{6}\right] \quad (9)$$

where $\varepsilon_{ij} = (\varepsilon_i\varepsilon_j)^{1/2}$ and $\rho_{ij} = (\rho_i\rho_j)^{1/2}$ and the parameter values are listed in Table 2. Note that both the Lennard-Jones expression (eq 9) and the combination rules of OPLS are slightly different from the CHARMM potential (eq 8). The temperature was maintained at 1000 K. Both NVT and NPT simulations (P = 1000 atm) were run for comparison. NPT runs began with energy minimization of 1000 $ThCl_4$ molecules arranged in a 10 × 10 × 10 box with a lattice spacing of 8.0 Å and an intramolecular Th−Cl distance of 2.8 Å. NVT runs began with the final positions, velocities, and volume of the constant pressure SPME simulation. Commensurate with larger interparticle separations than for NaCl, longer cutoffs (15 Å, 18 Å, 21 Å, and 24 Å) were used, neighbor list radii were 3 Å longer than the cutoffs, and the Ewald radius was 21 Å. Trajectories were propagated for 10 ns and coordinates recorded every 20 ps. The first 5 ns of NPT and the first 2 ns of NVT runs were excluded from analysis.

LEWIS water was simulated under similar MD conditions, except for a shorter time step of 0.2 fs and a lower temperature of 300 K. The 9 Å cutoff SPME run used a cubic box of 500 water molecules (edge length ∼ 24.7 Å). The 12 Å cutoff SF run used a larger box (edge length ∼ 36 Å) of 1500 molecules. Due to the relatively small time step and low temperature, the neighbor lists were updated only every 100 steps. The large water box was run for 250 ps, while all others were run for 1 ns. The first 200 ps of each run were excluded from analysis.

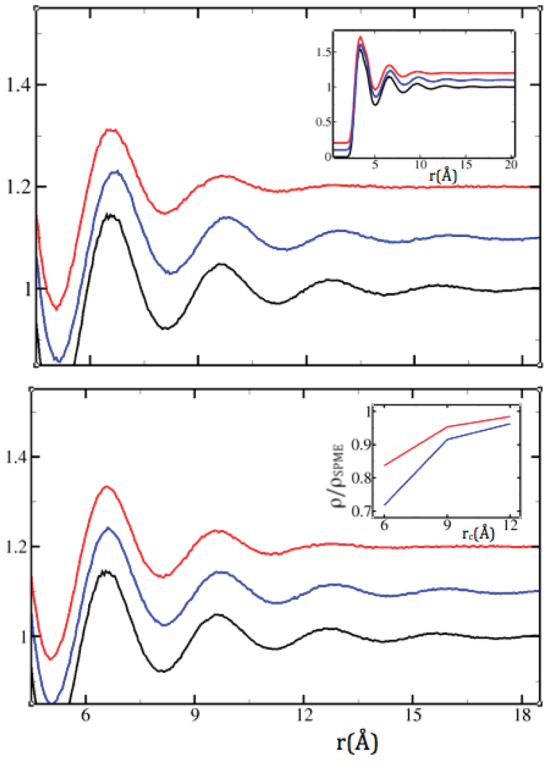

Figure 3. The SPME Na^+-Na^+ radial distribution function (black) compared to the (vertically translated) results obtained using SF (red) and SFG (blue), in the NPT ensemble with r_c = 9 Å (top) and r_c = 12 Å (bottom). The inset in the top panel shows the full radial distribution functions. The inset in the lower panel shows the convergence to 1 of the ratios of the predicted densities from NPT simulations to the SPME value (2.486 g/cm^3), with increasing cutoff radius (6, 9, and 12 Å). Peaks beyond the cutoff are better preserved with SFG. This occurs at the expense of a mild outward shift that is reduced with the longer cutoff.

RESULTS

Our LEWIS model for water exhibits dramatic artifacts in the $O^{6+}-O^{6+}$ correlations with the SF method. The prominent signature of SF is the presence of an artificially dense shell just inside the cutoff with a depletion layer just beyond (Figure 2). The associated peak and valley in the radial distribution are distinctive and become more prominent with smaller cutoffs. In the case of a 9 Å cutoff, the artifact peak is higher than the physical second and third neighbor peaks. In fact, the latter are pushed inward and become ordered by the artificial layer so that the hydrogen bond network is restructured. For a larger cutoff of 12 Å, the problem is less dramatic, yet the artifact is still significant. On the other hand, SFG resolves this abnormality already for r_c = 9 Å and reproduces the Ewald structure to a reasonable accuracy. For the present model, SPME takes about 8−9% longer on a parallel machine with 16 virtual cores.

In molten NaCl, neither SF nor SFG causes a distinct cutoff layer analogous to the LEWIS water artifact. However, SF harshly suppresses order beyond the cutoff, whereas SFG reproduces it (Figure 3). On the other hand, both the SF and SFG softening methods underestimate density with decreasing cutoff, SFG more so than SF (Figure 3, bottom panel inset).

As charge magnitudes increase, the artifact around the SF cutoff re-emerges. In $ThCl_4$, the effect is very similar to that in the LEWIS

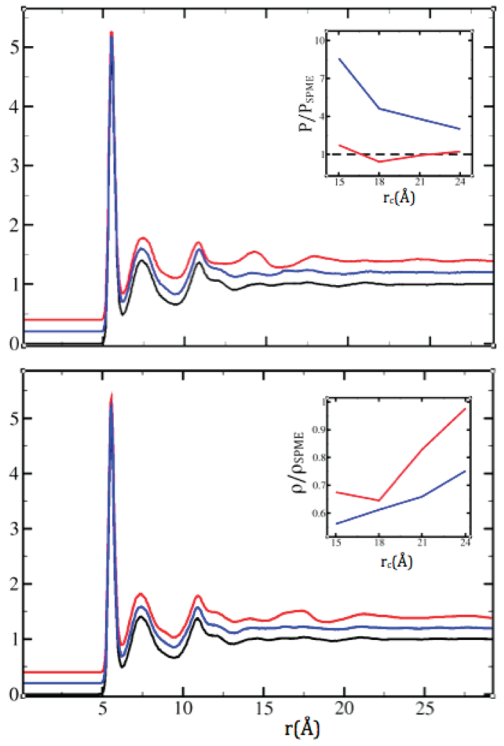

Figure 4. Simulations of $ThCl_4$. The SPME $Th^{4+}-Th^{4+}$ radial distribution function (black) compared to the (vertically translated) results obtained using SF (red) and SFG (blue), in the NVT ensemble with r_c = 15 Å (top) and r_c = 18 Å (bottom). The artifact layer in SF is still present with the longer cutoff, but less distinct. Insets show the dependence on the cutoff distance (15, 18, 21, and 24 Å) of the pressure in NVT simulations (top) and the density in NPT simulations (bottom) relative to the SPME values (590.5 bar and 3.011 g/cm^3, respectively).

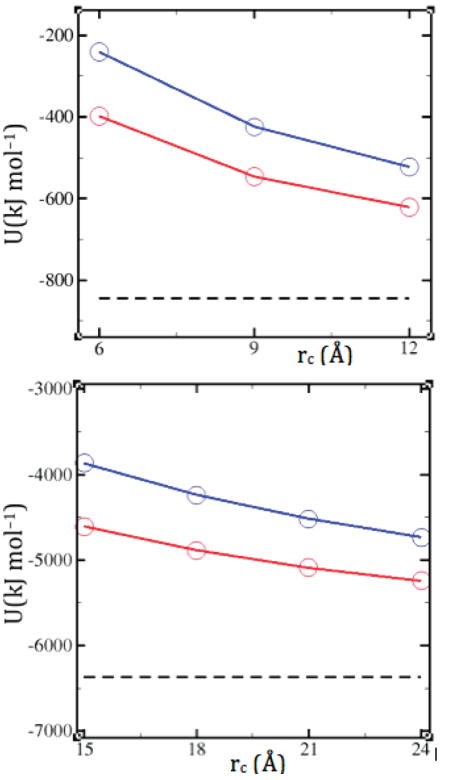

Figure 5. Total energy per salt molecule (kJ/mol) as a function of cutoff distance in NPT simulations of molten NaCl (top) and molten $ThCl_4$ (bottom). Cohesion is reduced by both SF (red) and SFG (blue), as compared to SPME (dashed black line).

water case, in the sense that it appears only in the $Th^{4+}-Th^{4+}$ correlations and becomes more pronounced and localized at shorter cutoffs (Figure 4). SFG lifts this abnormality in the structure. However, it does so at the expense of an underestimation of the density in NPT simulations or an overestimation of the pressure in NVT simulations (Figure 4 insets). Nevertheless, at constant volume, SFG predicts a structure that is virtually identical to SPME already at a cutoff below the Ewald radius (Figure 4, bottom panel).

DISCUSSION

This work provides evidence that, even in extreme systems, a pairwise compensation scheme can reproduce results similar to those obtained with conventional infinite lattice sums that are typically more CPU-intensive and more difficult to parallelize. When used in conjunction with neighbor lists and cell domain decomposition, pairwise methods can also offer linear scaling with the number of particles N.[13,19] Currently, most mainstream lattice-sum algorithms scale as $N \log(N)$,[9−11] which makes pairwise sums advantageous as systems grow in size.

We characterize three artifacts, two associated with SF and one with SFG. While SF can be a viable solution for weakly ionic liquids,[6] it results in an artificial layer just inside the cutoff as charges increase in magnitude. In our highly ionic water model, this layer appears in the homoionic correlations between +6 charged particles, and in molten $ThCl_4$ it appears between +4 charged particles. It does not appear in the other correlations of these liquids, or in any of the correlations in molten NaCl where the ionic charges are smaller. However, SF results in a different structural artifact in NaCl; i.e., long-range order is lost for small cutoffs. In contrast, SFG provides a reliable liquid structure in NVT simulations of $ThCl_4$. On the other hand, in NPT simulations, SFG causes more outward shifted correlations and greater underestimation of the density than SF. However, it is notable that in our strongly ionic water model, SFG obtains the Ewald density already at a cutoff of 9 Å. While this radius is small for an ionic liquid, it is still ∼20-fold larger than the smallest (i.e., intramolecular) ion separation of ∼0.3−0.5 Å in this system. Ions of molten $ThCl_4$ are significantly less densely distributed, with nearest neighbor distances varying between 2.7 Å and 5.5 Å. The cutoffs considered in this system, while large in magnitude, remain small multiples of typical interion separations.

The observed outward correlation shifts, and related density underestimations (Figure 3, bottom panel inset, and Figure 4, bottom panel inset), can be rationalized by considering the corrected potentials in Figure 1. To the extent that the potentials that hold the system together are attenuated, less cohesion is expected (Figure 5). Thus, the greater potential softening in the n = 2 correction than in the n = 1 correction is consistent with the greater correlation shifts and density underestimations. Constant volume ensembles can circumvent this issue at the expense of elevated pressures (Figure 4, top panel inset). Another alternative may be reoptimization of the force field for use with the specific long-range correction, as has been done, e.g., for Ewald compatibility of water models.[32,33]

We arrived at SFG compensation (eqs 5 and 6), to address our own needs for a novel, highly ionic model of water. However, the demonstrated advantages in more conventional ionic systems indicate that the approach may be of wider benefit for the computational community.

AUTHOR INFORMATION

Corresponding Author
*E-mail: herzfeld@brandeis.edu.

ACKNOWLEDGMENT

We thank Mason Kramer for technical advice and for his initial exploration of SP. This work was supported by NIH grant R01EB001035. Additional computational support was provided by the Brandeis HPC.

REFERENCES

(1) Sagui, C.; Darden, T. A. Molecular dynamics simulations of biomolecules: Long-range electrostatic effects. *Annu. Rev. Biophys. Biomol. Struct.* **1999**, *28*, 155–179.

(2) Schreiber, H.; Steinhauser, O. Molecular Dynamics Studies of Solvated Polypeptides - Why the Cutoff Scheme Does Not Work. *Chem. Phys.* **1992**, *168*, 75–89.

(3) Schreiber, H.; Steinhauser, O. Cutoff Size Does Strongly Influence Molecular Dynamics Results on Solvated Polypeptides. *Biochemistry* **1992**, *31*, 5856–5860.

(4) Auffinger, P.; Beveridge, D. L. A Simple Test for Evaluating the Truncation Effects in Simulations of Systems Involving Charged Groups. *Chem. Phys. Lett.* **1995**, *234*, 413–415.

(5) Brooks, B. R.; Bruccoleri, R. E.; Olafson, B. D.; States, D. J.; Swaminathan, S.; Karplus, M. CHARMM - a Program for Macromolecular Energy, Minimization, and Dynamics Calculations. *J. Comput. Chem.* **1983**, *4*, 187–217.

(6) Toxvaerd, S.; Dyre, J. C. Communication: Shifted forces in molecular dynamics. *J. Chem. Phys.* **2011**, *134*, 081102.

(7) Sagui, C.; Darden, T. Multigrid methods for classical molecular dynamics simulations of biomolecules. *J. Chem. Phys.* **2001**, *114*, 6578–6591.

(8) Ewald, P. The Berechnung optischer und elektrostatischer Gitterpotentiale. *Ann. Phys.* **1921**, *369*, 253–287.

(9) Toukmaji, A. Y.; Board, J. A. Ewald summation techniques in perspective: A survey. *Comput. Phys. Commun.* **1996**, *95*, 73–92.

(10) Darden, T.; York, D.; Pedersen, L. Particle Mesh Ewald - an N Log(N) Method for Ewald Sums in Large Systems. *J. Chem. Phys.* **1993**, *98*, 10089–10092.

(11) Essmann, U.; Perera, L.; Berkowitz, M. L.; Darden, T.; Lee, H.; Pedersen, L. G. A Smooth Particle Mesh Ewald Method. *J. Chem. Phys.* **1995**, *103*, 8577–8593.

(12) Wolf, D.; Keblinski, P.; Phillpot, S. R.; Eggebrecht, J. Exact method for the simulation of Coulomb systems by spherically truncated, pairwise 1/r summation. *J. Chem. Phys.* **1999**, *110*, 8254–8282.

(13) Allen, M. P.; Tildesley, D. J. Some tricks of the trade. In *Computer Simulation of Liquids*; Oxford University Press: New York, 1987; pp 145−146.

(14) Zahn, D.; Schilling, B.; Kast, S. M. Enhancement of the Wolf damped Coulomb potential: Static, dynamic, and dielectric properties of liquid water from molecular simulation. *J. Phys. Chem. B* **2002**, *106*, 10725–10732.

(15) Stoddard, S. D.; Ford, J. Numerical Experiments on Stochastic Behavior of a Lennard-Jones Gas System. *Phys. Rev. A* **1973**, *8*, 1504–1512.

(16) Barker, J. A. Reaction Field, Screening, and Long-Range Interactions in Simulations of Ionic and Dipolar Systems. *Mol. Phys.* **1994**, *83*, 1057–1064.

(17) Alper, H.; Levy, R. M. Dielectric and Thermodynamic Response of a Generalized Reaction Field Model for Liquid-State Simulations. *J. Chem. Phys.* **1993**, *99*, 9847–9852.

(18) Tironi, I. G.; Sperb, R.; Smith, P. E.; van Gunsteren, W. F. A Generalized Reaction Field Method for Molecular Dynamics Simulations. *J. Chem. Phys.* **1995**, *102*, 5451–5459.

(19) Fennell, C. J.; Gezelter, J. D. Is the Ewald summation still necessary? Pairwise alternatives to the accepted standard for long-range electrostatics. *J. Chem. Phys.* **2006**, *124*, 234104.

(20) Berendsen, H. J. C.; Grigera, J. R.; Straatsma, T. P. The Missing Term in Effective Pair Potentials. *J. Phys. Chem.* **1987**, *91*, 6269–6271.

(21) Kale, S.; Herzfeld, J.; Dai, S.; Blank, M. Lewis-inspired representation of dissociable water in clusters and Grotthuss chains. *J. Biol. Phys.* **2011**, DOI: 10.1007/s10867-011-9229-5.

(22) Levitt, M.; Hirshberg, M.; Sharon, R.; Daggett, V. Potential-Energy Function and Parameters for Simulations of the Molecular-Dynamics of Proteins and Nucleic-Acids in Solution. *Comput. Phys. Commun.* **1995**, *91*, 215–231.

(23) van der Spoel, D.; Lindahl, E.; Hess, B.; Groenhof, G.; Mark, A. E.; Berendsen, H. J. C. Gromacs: Fast, Flexible, and Free. *J. Comput. Chem.* **2005**, *26*, 1701–1718.

(24) Humphrey, W.; Dalke, A.; Schulten, K. VMD: Visual molecular dynamics. *J. Mol. Graphics* **1996**, *14*, 33–38.

(25) Beglov, D.; Roux, B. Finite Representation of an Infinite Bulk System - Solvent Boundary Potential for Computer Simulations. *J. Chem. Phys.* **1994**, *100*, 9050–9063.

(26) MacKerell, A. D.; Bashford, D.; Bellott, M.; Dunbrack, R. L.; Evanseck, J. D.; Field, M. J.; Fischer, S.; Gao, J.; Guo, H.; Ha, S.; Joseph-McCarthy, D.; Kuchnir, L.; Kuczera, K.; Lau, F. T. K.; Mattos, C.; Michnick, S.; Ngo, T.; Nguyen, D. T.; Prodhom, B.; Reiher, W. E.; Roux, B.; Schlenkrich, M.; Smith, J. C.; Stote, R.; Straub, J.; Watanabe, M.; Wiorkiewicz-Kuczera, J.; Yin, D.; Karplus, M. All-atom empirical potential for molecular modeling and dynamics studies of proteins. *J. Phys. Chem. B.* **1998**, *102*, 3586–3616.

(27) MacKerell, A. D.; Banavali, N.; Foloppe, N. Development and current status of the CHARMM force field for nucleic acids. *Biopolymers* **2001**, *56*, 257–265.

(28) Bussi, G.; Donadio, D.; Parrinello, M. Canonical sampling through velocity rescaling. *J. Chem. Phys.* **2007**, *126*, 014101.

(29) Berendsen, H. J. C.; Postma, J. P. M.; van Gunsteren, W. F.; Dinola, A.; Haak, J. R. Molecular Dynamics with Coupling to an External Bath. *J. Chem. Phys.* **1984**, *81*, 3684–3690.

(30) Jorgensen, W. L.; Maxwell, D. S.; TiradoRives, J. Development and testing of the OPLS all-atom force field on conformational energetics and properties of organic liquids. *J. Am. Chem. Soc.* **1996**, *118*, 11225–11236.

(31) Jensen, K. P.; Jorgensen, W. L. Halide, ammonium, and alkali metal ion parameters for modeling aqueous solutions. *J. Chem. Theory Comput.* **2006**, *2*, 1499–1509.

(32) Price, D. J.; Brooks, C. L. A modified TIP3P water potential for simulation with Ewald summation. *J. Chem. Phys.* **2004**, *121*, 10096–10103.

(33) Rick, S. W. A reoptimization of the five-site water potential-(TIP5P) for use with Ewald sums. *J. Chem. Phys.* **2004**, *120*, 6085–6093.